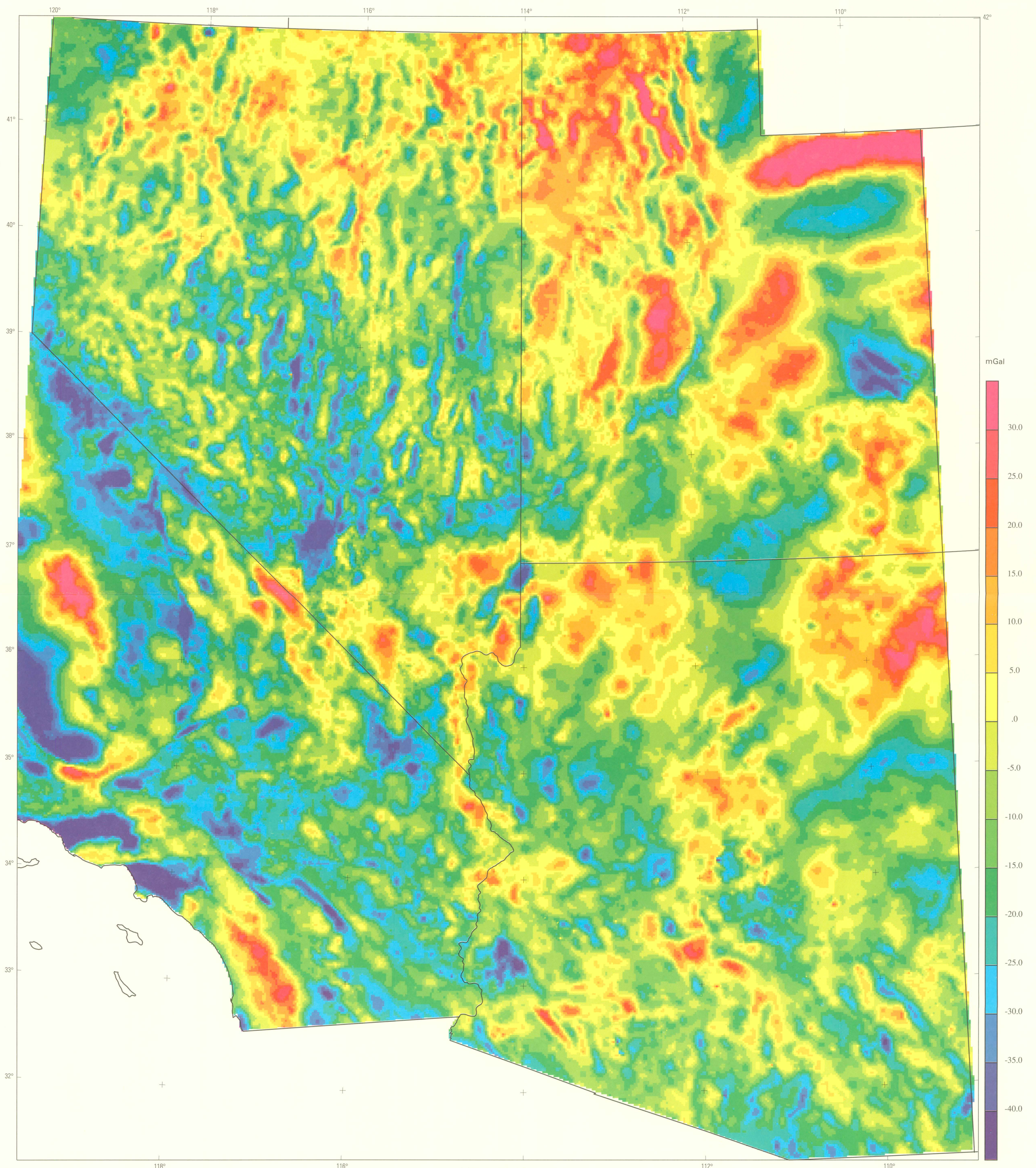

Map A. Map showing isostatic residual gravity anomalies

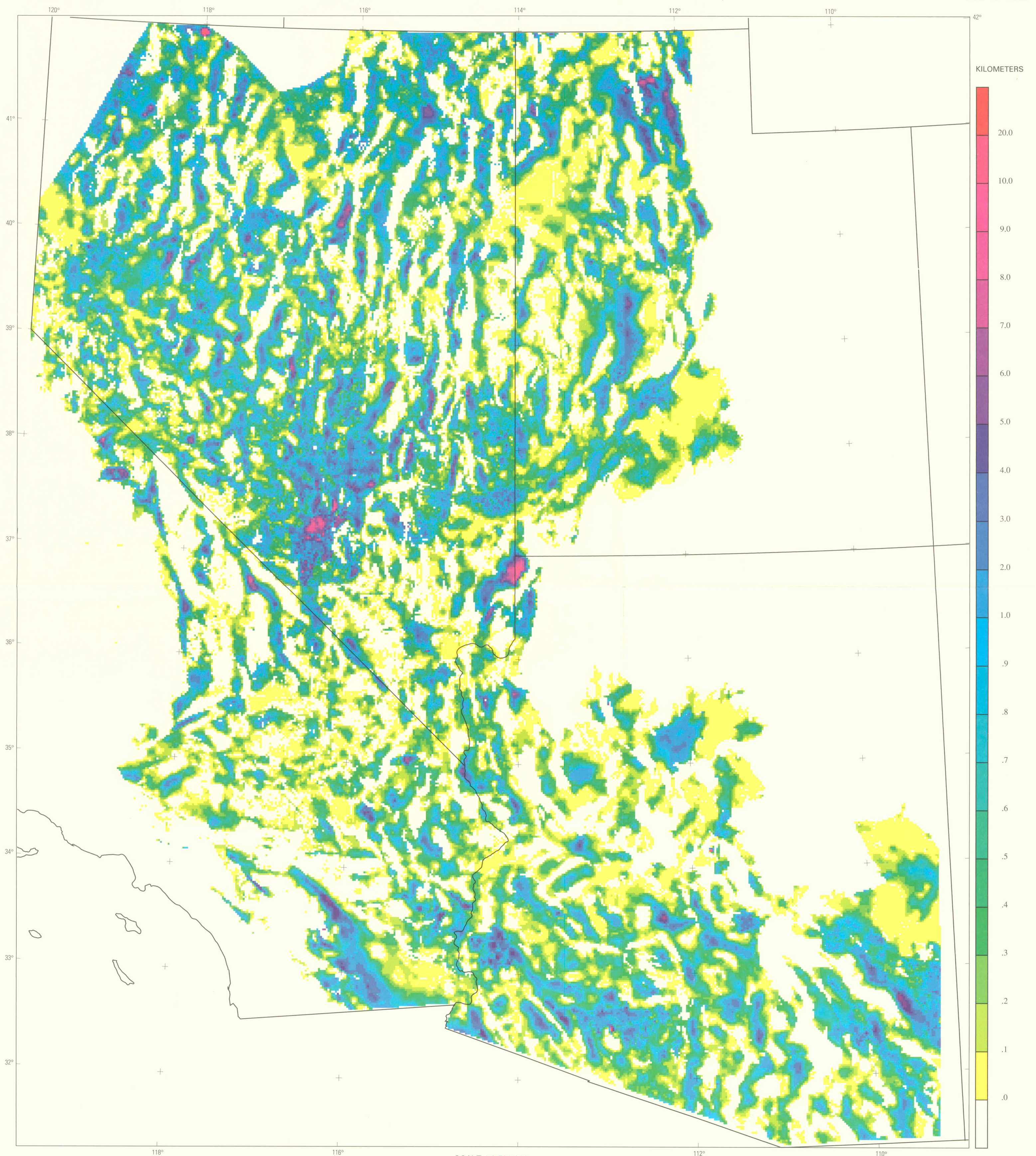

Map C. Map showing basin depths from gravity model

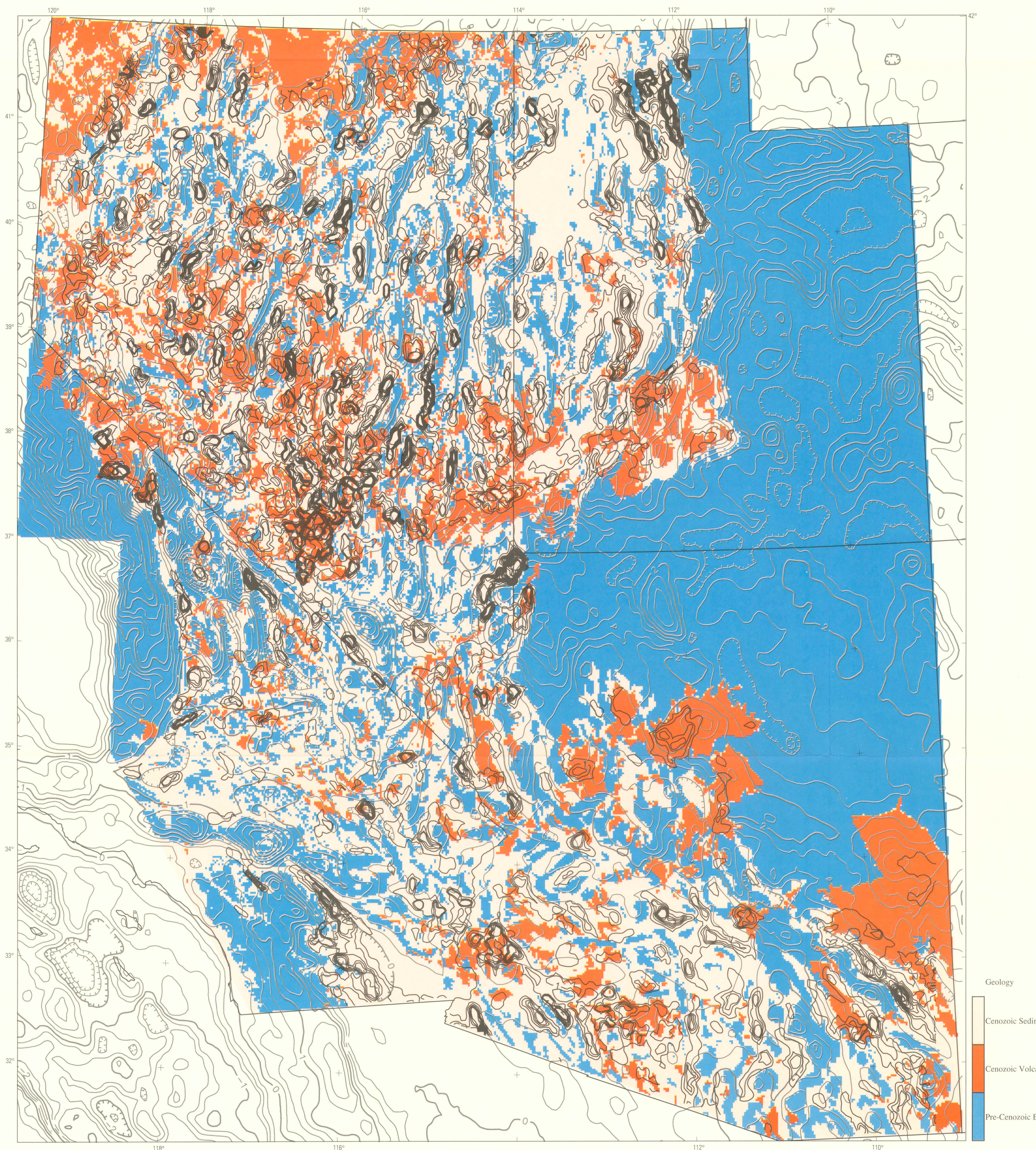

EXPLANATION

Topographic contour—Contour interval 0.25 km.
Hachures indicate enclosed area of lower topography

Basin depth—Contour interval 0.5 km

Map B. Map showing geology, topography, and modeled basin depths

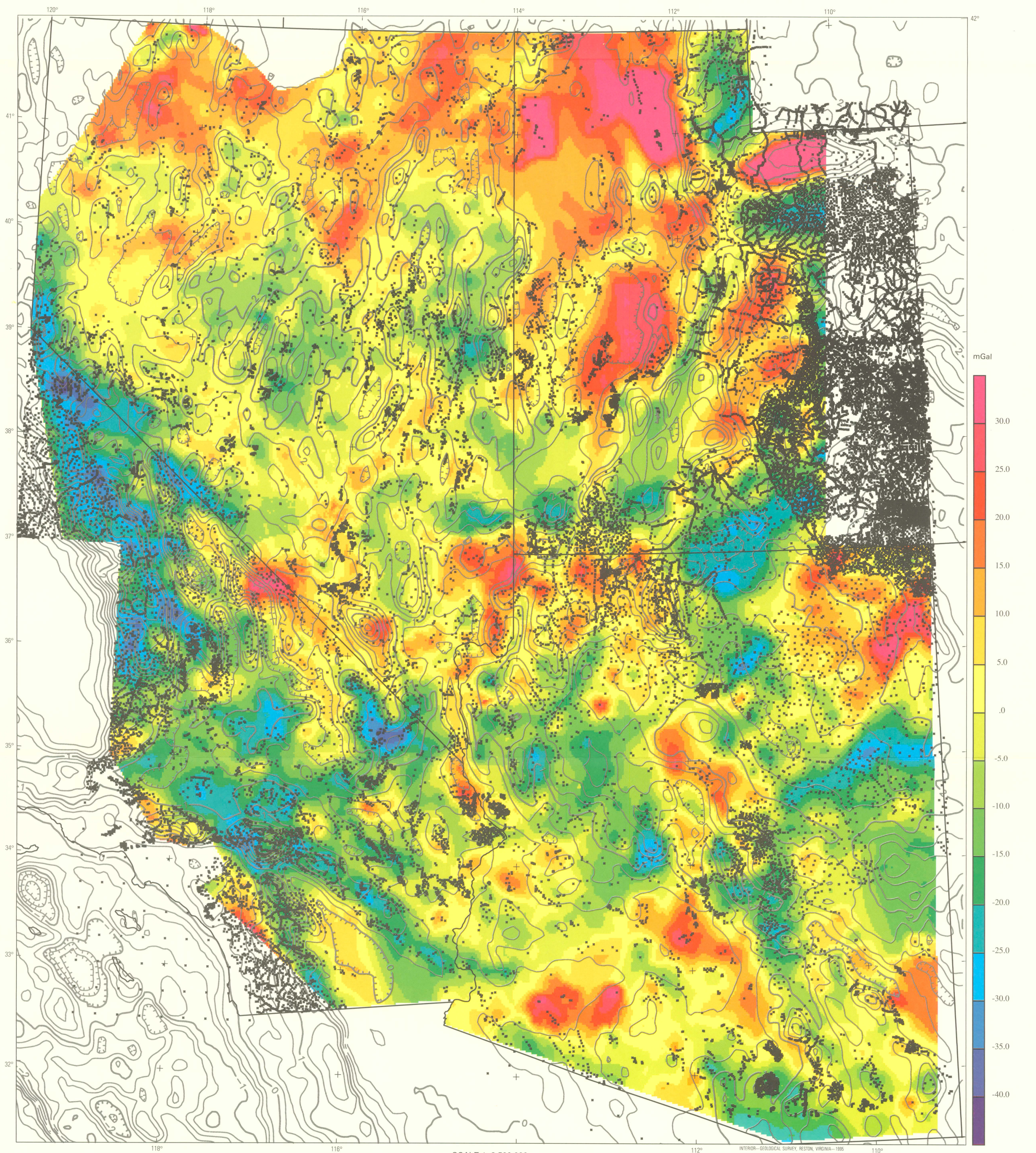

EXPLANATION

Topographic contour—Contour interval 0.25 km.
Hachures indicate enclosed area of lower topography

Basement gravity station

Map D. Map showing basement residual gravity anomalies and topography

INTERIOR—GEOLOGICAL SURVEY, RESTON, VIRGINIA—1995

Edited by F. Craig Brunstein
Graphic design by Virginia D. Scott
Cartography by Joseph A. Romero
Digital map production by Eugene G. Ellis
Manuscript approved for publication July 7, 1994

Digital geologic data prepared with Adobe Illustrator 5.5 running under System 7.0 on a Macintosh personal computer

ABSTRACT

These maps show gravity values and modeled basin depths in the Basin and Range Province, Western United States. The four maps are (A) isostatic residual gravity anomaly, (B) digital geology, topography, and basin depth, (C) basin depths from gravity model, and (D) basement residual gravity anomaly. An iterative, three-dimensional separation technique, constrained by digital geology and density-depth information from borehole gravimetry and density logs, was used to model basin geometry and isolate basement residual gravity anomalies. The basement residual gravity anomalies primarily reflect density variations in the pre-Cenozoic rocks of the upper crust. The basin depth model provides a synoptic view of the subsidence patterns of Cenozoic extension; in detail, however, the depths shown on the maps are dependent on the simple density-depth functions used for Cenozoic sedimentary and volcanic rocks.

INTRODUCTION

The maps in this report show most of the Basin and Range Province (Eaton, 1982), a region that has experienced widespread Cenozoic extension. As a result of tectonic, volcanic, and geomorphic processes accompanying extension, the pre-Cenozoic basement of about 80 percent of the Basin and Range Province is obscured by sedimentary and volcanic cover deposits. To learn about the crustal structure and evolution of this zone of extension, it is necessary to look beneath this cover. Analysis of gravity data allows estimation of the shape and extent of the Cenozoic basins in three dimensions, and allows us to examine large-scale density heterogeneities in the pre-Cenozoic basement. The method used here is derived from a method (Jachens and Moring, 1990) developed for mineral resource analysis in Nevada.

The large density contrast between the pre-Cenozoic basement rocks and the overlying Cenozoic volcanic and sedimentary cover rocks causes variation in basin depth to have a strong gravity signature. The mapped contact between the basement and cover rocks constrains the zero-depth contour of the basin depth model. This spatial constraint, together with an assumed density-depth function for the Cenozoic fill, allows the separation of basement and basin gravity effects. The resulting basement residual gravity map (map D) shows anomalies that predominantly reflect large-scale lateral density heterogeneities in the pre-Cenozoic basement.

The depth-to-basement model (shown on maps B and C) is a by-product of the basement-basin gravity separation process. The modeled depths depend on the chosen density-depth function. The depth-to-basement model is useful for comparing basin geometries, but the uncertainties in the conversion of basin gravity anomalies to depth must be kept in mind. The depth-to-basement model also serves as a check on the gravity inversion, because it can be compared with independent depth estimates from borehole data. The depth-to-basement map displays the subsidence patterns caused by Cenozoic extension in the Basin and Range.

INPUT DATA

ISOSTATIC RESIDUAL GRAVITY DATA

The isostatic residual gravity anomaly (map A) is used in this study because it is primarily sensitive to geologic bodies in the upper parts of the crust (Simpson and others, 1986). The isostatic residual anomaly is derived from the Bouguer gravity anomaly by the subtraction of a topography-based regional field. This regional field is the calculated gravitational effect of the topographic roots required for local (Airy) isostatic compensation (Simpson and others, 1986).

The isostatic residual gravity data set is a combination of gravity data from several state compilations: California (about 37,000 data points; Snyder and others, 1981), Nevada (about 71,000 data points; Saltus, 1988a, b, c), and Utah (about 42,000 data points; Cook and others, 1989); and Arizona (about 20,000 data points) from the U.S. Department of Defense, Defense Mapping Agency gravity data base [available from the National Geophysical and Solar-Terrestrial Data Center, Boulder, Colorado 80303]. The isostatic corrections were calculated using the following model parameters: Bouguer reduction density (equal to the topographic load density) of 2.67 g/cm^3, depth to root at sea level of 30 km, and density contrast across the root of 0.35 g/cm^3. The isostatic residual gravity field is insensitive to the exact choice of these parameters (Saltus, 1984; Simpson and others, 1986).

DIGITAL GEOLOGY

A three-unit digital geology model was created from mapped geology of Arizona (Reynolds, 1988), Utah (Stokes, 1963; Hintze, 1962), Nevada (Stewart and Carlson, 1978), and California (Jennings, 1977). The units are:

1. Pre-Cenozoic basement rock
2. Cenozoic volcanic rocks
3. Cenozoic sedimentary cover, primarily Quaternary alluvium

Map B shows the distribution of each of these units. Only about 20 percent of the Basin and Range Province is pre-Cenozoic outcrop.

The geology was manually digitized from maps with scales of 1:250,000 (Utah and California), 1:500,000 (Nevada), and 1:1,000,000 (Arizona). Polygons that enclose the outcrops were constructed for the pre-Cenozoic basement and Cenozoic volcanic rock units. The parts of the map not enclosed by these polygons represent areas of Cenozoic sedimentary cover. The basement polygons were used to extract gravity stations on basement outcrop. The geology polygons contain more detail than is shown on map B.

DENSITY-DEPTH FUNCTIONS

The third data set for this study is the assumed density-depth functions for Cenozoic deposits (table 1). The functions are from Jachens and Moring (1990). The density-depth function for Cenozoic sediments is based mainly on borehole gravimetry and gamma-gamma density logs from deep holes in central Nevada (Healey, 1970; Healey and others, 1984), northern Nevada (Robbins and others, 1985), and Arizona (Oppenheimer, 1980; Tucci and others, 1982). The Cenozoic volcanic rock density-depth function is based mainly on measurements of surface samples (Healey, 1970; Ponce, 1981; Okaya and Thompson, 1985).

The density-depth functions (table 1) follow the general trend of increasing density with depth as suggested by the subsurface density data. A more sophisticated model might fit the increase with depth to an exponential or hyperbolic function (for example, Cordell, 1973; Litinsky, 1989), but, given the expected resolution of the depth model, the extra complication is not warranted. In both density-depth functions all deposits deeper than 1.2 km are assumed to have a constant density contrast with basement (a simplification that is helpful for the stability of the inversion process). If deep basin-fill densities approach basement density then the depth of the basin cannot be determined from gravity data. Also, since most of the basin deposits in the Basin and Range are apparently thinner than 600 m, the deep density contrast assumption is only applicable to a small part of the map. Subsurface density information from regions of Cenozoic volcanic rock outcrop is scarce, so the density-depth function for Cenozoic volcanic rocks is defined on the basis of the observed average surface densities of volcanic rocks and from inferred densities from seismic wave velocities (Zbur, 1963; Okaya and Thompson, 1985).

METHOD OF FIELD SEPARATION AND INVERSION

The correlation in pattern between the geologic map (map B) and the isostatic residual gravity anomaly map (map A) is striking; the sediment-filled basins of the Basin and Range produce a distinctive set of north-south-trending lows. Cenozoic volcanic centers also produce gravity lows, the most notable over the southwestern Nevada volcanic field that includes the Silent Canyon caldera (Healey, 1968; Kane and others, 1981). The goal of the basin-basement field separation is to remove these lows so that only the gravity variations caused by density variations in the pre-Cenozoic basement remain. To accomplish this field separation, a model of basin depths is constructed. The method described here is modified from the original method of Jachens and Moring (1990).

STEP 1: LOCATE GRAVITY OBSERVATIONS MADE ON BASEMENT OUTCROP AND CONSTRUCT AN INITIAL ESTIMATE OF THE BASEMENT GRAVITY GRID

The first step of the basin-basement separation procedure is to select only those gravity stations that are on basement outcrop and construct from them a gravity grid. A basement gravity station is identified by determining whether it is inside one of the pre-Cenozoic basement polygons of the digital geology model. The distribution of these basement gravity stations (shown on map D) is a fundamental limitation on the accuracy of the resulting basement gravity grid. This distribution is a function of both the geology (map B) and the data coverage. Large gaps between basement gravity stations present a special challenge to the gridding procedure.

The gridding procedure begins with a computer program (Webring, 1981) that uses a minimum curvature algorithm (Briggs, 1974) to construct a grid from the basement gravity values. Minimum curvature works well when tightly constrained by data points, but it can produce undesirable results when allowed to extrapolate too far. If a steep gradient is found between two adjacent data points at the edge of a region of no data (for example, at the edge of a large basin), the minimum curvature algorithm can extrapolate a large bulge into that part of the grid. This tendency can be fatal to the iterative scheme used here for basin-basement separation, so it is necessary to modify the minimum curvature algorithm in regions of significant extrapolation.

To address this problem, Jachens and Moring (1990) used a technique of successive approximation in which they began with a grid that has large row and column spacing, and then they worked down to smaller and smaller grid spacing. At each successive gridding step the smooth grid points created in the previous step were converted to synthetic data points and added to the input data for the next step. This procedure was successful in preventing unstable inversion in Nevada and southern California, but the procedure is taxed in regions that have large data gaps such as northwestern Utah. In addition, the successive gridding method is slow because it requires many runs of the gridding program to construct a single grid.

Another solution to the problem is used here. Rather than use successive grid steps to limit excessive minimum curvature extrapolation, a different method of extrapolation is used in the large regions of sparse data coverage; those regions of the grid are filled using linear interpolation. The grid is constructed in two steps, first the minimum curvature algorithm is used to create the entire grid at the final gridding interval (2 km for this study), then all regions of that grid that are more than two grid cells removed from a data point are replaced with values interpolated on a plane fit through the nearest neighboring stations. This grid is a more conservative estimate of the basement gravity field than that obtained by Jachens and Moring (1990), but our results in Nevada are similar to those of Jachens and Moring (1990).

The basement gravity grid constructed from these stations still contains some basin-induced effects, however, because measurements near the edge of a basin are affected by the gravity low from that basin. The rest of the procedure is designed to remove these basin-induced effects from the basement gravity map. One reason for the stability of the inversion procedure is that these basin-induced effects are small in the Basin and Range. This is mostly a result of the generally shallow flanks (pediments) of the basins and the elongate shape of the basins. If the basin-bounding faults were closer to the range fronts then the effects would be much larger.

STEP 2: BASIN-BASEMENT SEPARATION AND CONSTRUCTION OF A BASIN DEPTH MODEL

The second step of the basin-basement separation procedure is to obtain an estimate of the gravity field caused by Cenozoic sedimentary and volcanic cover and then invert that field for basin depth. If G_r is the isostatic residual gravity grid, G_b is the basement gravity grid, and G_c is a grid of the gravity anomaly caused by the sedimentary and volcanic cover rocks, then

$$G_r = G_b + G_c$$

Using the basement grid G_b from step 1, G_c is obtained by subtraction:

$$G_c = G_r - G_b$$

The basin grid G_c is then converted to a basin depth grid D_c using a one-dimensional point-wise calculation and the two density-depth functions discussed above, one for volcanic rocks and one for sedimentary cover. At each point in the grid, basin depth is given by

$$D_c = \sum_{i=1}^{n} T_i$$

where n is the number of layers in the density-depth function (four in this model) and T_i is the thickness of the ith layer at each point. The layer thicknesses are such that

$$G_c = 2\pi\gamma \sum_{i=1}^{n} \Delta\rho_i T_i$$

where γ is the gravitational constant, $\Delta\rho_i$ is the density contrast of the ith layer of the density depth model, and $0 \le T_i \le Tm_i$ where Tm_i is the maximum thickness of a layer in the depth model. The nth layer of the model has no maximum thickness. Because of the one-dimensional approximation, the depth grid D_c will generally underestimate the true basin depth.

STEP 3: THREE-DIMENSIONAL CORRECTION FOR BASIN EFFECTS

The next step of the procedure is to make a three-dimensional forward calculation of the predicted basin gravity anomaly Gc_c from the depth model D_c, and use this calculation as an estimate of the basin effect at basement gravity measurement sites. The calculation is done by the method of Parker (1972) using a computer program by R.W. Simpson (U.S. Geological Survey, written commun., 1993). Basin gravity anomalies are interpolated from Gc_c at the basement gravity measurement sites. These anomalies are subtracted from the isostatic residual gravity anomalies to obtain a better estimate of the uncontaminated basement gravity value. Once the basement gravity values have had this correction applied, they can be gridded again to obtain a better estimate of G_b.

STEP 4: ITERATE STEPS 2 AND 3

The revised basement gravity grid G_b is then used to repeat step 2 and is subtracted from the isostatic residual gravity G_r to obtain a new gravity anomaly G_c. For this study 6 iterations were sufficient to produce small differences between successive estimates of the basement gravity field G_b.

WHY THE PROCEDURE WORKS

The basin-basement separation procedure is potentially unstable; if the basin depth is significantly overestimated at any iteration, then subsequent iterations will make increasingly deeper estimates (an increasingly greater D_c). It is easy to see why this will happen; a gross overestimate of basin depth D_c in step 2 will cause the calculated basin field Gc_c of step 3 to overestimate the gravity low caused by the basin and this overestimate will, in turn, lead to an artificial increase in the gravity values of measurements flanking the basin. Then, when these contaminated basement stations are gridded for the next iteration they will cause an even larger estimate of G_c and the problem will become worse.

Several factors contribute to the success of the basin-basement separation technique despite this possible instability. An important factor is the general character of the basins in the Basin and Range, namely their relatively large near-surface density contrast and shallow average depths. These characteristics have the important consequence that they limit the areal extent of the basin gravity lows. Another important factor is a typical basin geometry that consists of shallow basin depths (pediments) along the range fronts and deepest basin levels offset toward the centers of the basins. This offset of the deeper levels also helps limit the effect of basin lows on gravity observations in the adjacentt ranges. The assumption of a constant density contrast for Cenozoic deposits deeper than 1.2 km in both of the density-depth functions also contributes to the stability of the method. As the density contrast decreases with depth, it is necessary to use a greater increment in basin depth to achieve an equal gravity effect; this tendency could increase without limit for a density-depth function that approached zero contrast with depth.

POSSIBLE PROBLEMS

As outlined above, the iterative modeling procedure used in this study is based on some simplifying assumptions (perhaps the least certain of which are the density-depth functions). In addition, the stability of the separation of basin and basement gravity is dependent on the good correlation of basin gravity anomalies with the mapped area of the basins and the tendency of the basins to have shallow flanks. Places where the assumptions and typical basin geometries do not apply can present difficulties to the method.

Problems with the density-depth function will affect primarily the conversion of basin gravity anomaly to depth, not the separation of basin and basement gravity. For example, a big discrepancy between model basin depth and actual basin depth will arise in basins with significant low-density evaporite accumulation. The low density of salt deposits compared with the density-depth functions in table 1, will lead to model depths that overestimate actual depths. This may affect model depths in northern Utah, particularly in the Great Salt Lake basin.

As discussed previously, extrapolations between gravity stations on widely-spaced basement outcrops present a difficulty to the method. An extreme example of this problem is on the northern boundary of the study area in Nevada and Utah. There the Cenozoic volcanic rocks related to the Snake River Plain blanket the map, leaving no pre-Cenozoic outcrop to anchor the basement gravity grid.

If a large basement slide block suspended within basin fill strata is mistaken as basement outcrop, the basin depth will be incorrectly set to zero there. This will cause part of the basin gravity low to be assigned to the basement gravity field. At the scale of the current study this is probably not a significant problem, but it must be kept in mind for more detailed studies of individual basins.

A related problem can occur in regions where the Cenozoic surficial geology is not representative of the deeper rocks. An example is a thin layer of Cenozoic volcanic rocks that overlay a primarily sedimentary section or vice-versa. The similarities in the 0.6 to >1.2 km depth range of the two density-depth functions help minimize this problem.

Another problem is that density variation in the basement beneath a basin could be interpreted instead to reflect the geometry of the basin. This could happen if a low-density felsic intrusion underlies a basin. The low could be attributed to greater basin depth and the basement gravity low associated with the intrusion could be missed. Basement gravity anomalies that have wavelengths smaller than the spacing between outcrop stations are beyond the resolution of the methods in this study.

BASEMENT GRAVITY ANOMALIES

The basement residual gravity map (map D) displays medium-scale crustal density variations, primarily from sources in the mid to upper crust. A fundamental limitation on the resolution of the map is the basement gravity station coverage (x's on map D). Anomalies that have wavelengths less than or equal to basin widths are poorly defined. However, anomalies that have wavelengths greater than one or two basin widths are well defined. As can be seen on the geologic map (map B), the entire Colorado plateau has been regarded as basement outcrop for the purposes of this report. Thus, for the Colorado plateau, the basement gravity map is identical to the isostatic residual gravity map, except for some loss of short wavelength information caused by regridding of a coarser grid interval.

BASIN DEPTH MODEL

The depth-to-basement map (black lines on map B, colors on map C) is an inversion of the gravity data using the simple density-depth functions given in table 1 and using constraints from surface geology. The calculated depths are clearly dependent on the chosen density-depth functions and should be considered significant in a relative rather than absolute sense, particularly for depths greater than about 5 km. Comparisons with independent depth-to-basement determinations from boreholes show significant differences and suggest that, on average, depths may be slightly under-estimated, particularly in regions that have poor gravity station coverage in the basins.

Jachens and Moring (1990) found that depths calculated in Nevada agree well with depths-to-basement from 225 boreholes as deep as 1.2 km (70 percent of the depths agree within 200 m, and 85 percent agree within 300 m), but calculated depths are less reliable for depths greater than 1.2 km. Jachens and Moring (1990) used strict criteria for well selection; only those wells that were determined by the drillers to have penetrated basement and that had gravity stations within 2–3 km were selected.

Comparison of model depths with a less restricted set of borehole depths was done by Saltus (1991). Four different well data sets are used for the comparison, a Great Basin set of 164 points (from a U.S. Geological Survey computer data base maintained by the Oil and Gas Branch in Denver), a Utah set of 50 points (selected from Kerns, 1987), an Arizona set of 49 points (from the Arizona Oil and Gas Conservation Commission, 1989), and an Arizona subset of 7 points (from the Arizona Oil and Gas Conservation Commission, 1979). The Great Basin, Utah, and the small Arizona data sets contain depths to basement (either pre-Cenozoic strata identified as a formation top or the first high-density strata encountered beneath cover sediments). The main Arizona data set contains only total depths of wells that bottomed in pre-Cenozoic formations, so it represents depths greater than or equal to pre-Cenozoic basement. The agreement of these depths with the basin depth model is not as good as for the comparison given by Jachens and Moring (1990). The difference in fit is probably caused by the less restrictive borehole depth criteria used in our study. There is a clear tendency for the basin depth model to underestimate borehole depth to basement, particularly for wells shallower than 1.5 km. This is probably a reflection of data coverage in the basins; the use of conventional conservative gridding criteria (minimum curvature) will tend to cause a minimum estimate of the basinal gravity low in regions of poor data control and will thus lead to a minimum depth estimate. Part of the discrepancy is caused by mistaken basement depth estimates from drilling logs (Saltus, 1991). Another source of discrepancy is the coarse grid spacing used for the basin depth model; a two-kilometer grid was used for the modeling, so basin detail is limited to that resolution.

The initial goal of this comparison of model depths to depth to basement from borehole data was to use that information to revise the density-depth functions and revise the basin depth model. Based on the results of Jachens and Moring (1990) and examination of high quality subsets of the borehole data, it was determined that potential uncertainty in the widely scattered borehole depths was nearly as great as that in the basin depth model. At the scale of the maps in this study, modification of the density-depth function is not warranted by the comparisons. For detailed studies of individual basins where specific depth to basement or density-depth information is available, revision of the basin depth model is advisable. In that case, the separation of basin and basement gravity anomaly need not be redone, instead the final basin gravity field should be inverted again for depth. The separation of basin and basement gravity is much less model dependent than the inversion of basin gravity for depth.

Another check of the validity of the simple density-depth functions is comparison with a detailed analysis of basin depths in Arizona (Oppenheimer, 1980; Oppenheimer and Sumner, 1981; Sumner, 1985). Although two-dimensional gravity modeling was employed in that study, the detailed basin thickness map was well constrained by shallow borehole data for regions shallower than 600 m. The published 1-km-contour version of the Arizona study (Sumner, 1985) agrees well with the model developed here.

SUMMARY

A new three-dimensional technique produces a stable separation of the gravity field caused by Cenozoic basins and pre-Cenozoic basement in the Basin and Range. The technique uses geometric constraints from geologic mapping and density-depth functions inferred from borehole information. A basin depth model, created as part of the separation procedure, is dependent on the assumed density-depth functions. The iterative separation scheme has the potential to become unstable in regions with steep-sided basins or steep gradients in basement gravity. This possible instability is mitigated by careful control of excess extrapolation in the gridding process and by the tendency of the basins in the Basin and Range to have flanking pediments (regions of shallow depth to basement). Comparison of model basin depths with independent depths from boreholes shows significant disagreement and a tendency for shallow basin depths to be under-estimated in the model, but, in general, model depths follow the borehole depths. The resulting basement gravity map shows anomalies resulting from lateral density heterogeneities in the mid to upper crust, anomalies that may reflect the processes that accomplished Cenozoic extension (Saltus, 1991, chapter 5). The basin depth model provides a synoptic view of the geometry of Cenozoic extensional basins and provides constraints on the understanding of extension in the brittle upper crust (Saltus, 1991, chapter 6).

ACKNOWLEDGMENTS

John Mariano digitized detailed geology in the Mojave region. Bob Simpson got this all started with his modern revival of the isostatic residual gravity map in 1986. Careful reviews by David Ponce and David Daniels improved this work.

REFERENCES

Arizona Oil and Gas Conservation Commission, 1979, Oil and Gas Map 13, Structure Map of SE Arizona: Phoenix, State of Arizona, scale 1:500,000.
———1989, Well Location Map 4: Phoenix, State of Arizona, scale 1:666,666.
Briggs, I.C., 1974, Machine contouring using minimum curvature: Geophysics, v. 39, p. 39–48.
Cook, K.L., Bankey, V., Mabey, D.R., and DePangher, M., 1989, Complete Bouguer Gravity Anomaly Map of Utah: Utah Geological and Mineralogical Survey Map 122, scale 1:500,000.
Cordell, L., 1973, Gravity analysis using an exponential density depth function—San Jacinto Graben, California: Geophysics, v. 38, p. 684–690.
Eaton, G.P., 1982, The Basin and Range Province: Origin and tectonic significance: Annual Review of Earth and Planetary Sciences, v. 10, p. 409–440.
Healey, D.L., 1968, Application of gravity data to geologic problems at Nevada Test Site, *in* Eckel, E.B., ed., Nevada Test Site: Geological Society of America Memoir 110, p. 147–156.
———1970, Calculated in situ bulk densities from subsurface gravity observations and density logs, Nevada Test Site and Hot Creek Valley, Nye County, Nevada: U.S. Geological Survey Professional Paper 700–B, p. B52–B62.
Healey, D.L., Clutsom, F.G., and Glover, D.A., 1984, Borehole gravity meter surveys in drill holes USW G–3, UE–25p1 and UE–25c1, Yucca Mountain Area, Nevada: U.S. Geological Survey Open-File Report 84–672, 16 p.
Hintze, L.F., 1962, Geologic map of southwestern Utah: University of Utah, scale 1:250,000.
Jachens, R.C., and Moring, B.C., 1990, Maps of the thickness of Cenozoic deposits and the isostatic residual gravity over basement for Nevada: U.S. Geological Survey Open-File Report 90–404, 15 p.
Jennings, C.W., 1977, Geologic map of California with topographic contours: California Division of Mines and Geology, Geologic Data Map no. 2, scale 1:750,000
Kane, M.F., Webring, M.W., and Bhattacharyya, B.K., 1981, A preliminary analysis of gravity and aeromagnetic surveys of the Timber Mountain area, southern Nevada: U.S. Geological Survey Open-File Report 81–189, 40 p.
Kerns, R.L., Jr., 1987, Review of the petroleum activity of the Utah portion of the Great Basin; Cenozoic Geology of Western Utah—Sites for Precious Metal and Hydrocarbon Accumulations: Utah Geological Association Publication 16, p. 487–526.
Litinsky, V.A., 1989, Concept of effective density; Key to gravity depth determinations for sedimentary basins: Geophysics, v. 54, p. 1474–1482.
Okaya, D.A., and Thompson, G.A., 1985, Geometry of Cenozoic extensional faulting: Dixie Valley, Nevada: Tectonics, v. 4, p. 107–125.
Oppenheimer, J.M., 1980, Gravity modeling of alluvial basins in southern Arizona: Technical papers, Annual International Meeting and Exposition, Society of Exploration Geophysicists, no. 50, p. 255–335.
Oppenheimer, J.M., and Sumner, J.S., 1981, Gravity modeling of the basins in the Basin and Range province, Arizona: Arizona Geological Society Digest, v. 13, p. 111–116.
Parker, R.L., 1972, The rapid calculation of potential anomalies: Geophysical Journal of the Royal Astronomical Society of London, v. 31, p. 447–455.
Ponce, D.A., 1981, Preliminary gravity investigations of the Wahmonie Site, Nevada Test Site, Nye County, Nevada: U.S. Geological Survey Open-File Report 81–522, 64 p.
Reynolds, S.J., 1988, Geologic map of Arizona: Arizona Geological Survey Map 26, scale 1:1,000,000.
Robbins, S.L., Prudic, D.E., Schaefer, D.H., and Clutsom, F.G., 1985, Principal facts and density estimates for borehole gravity stations in three water wells located in Dixie and Paradise Valleys, Nevada: U.S. Geological Survey Open-File Report 85–426, 20 p.
Saltus, R.W., 1984, A description of colored gravity and terrain maps of the southwestern cordillera: U.S. Geological Survey Open-File Report 84–95, 8 p., 30 35mm slides.
———1988a, Gravity data for the state of Nevada on magnetic tape: U.S. Geological Survey Open-File Report 88–433, 20 p.
———1988b, Bouguer gravity anomaly map of Nevada: Reno, Nevada Bureau of Mines and Geology Map 94A, scale 1:750,000.
———1988c, Regional, residual, and derivative gravity maps of Nevada: Reno, Nevada Bureau of Mines and Geology Map 94B, scale 1:1,000,000.
———1991, Gravity and heat flow constraints on Cenozoic tectonics of the western United States cordillera: Stanford, Calif., Stanford University, Ph.D. thesis, 245 p.
Simpson, R.W., Jachens, R.C., Blakely, R.J., and Saltus, R.W., 1986, A new isostatic residual gravity map of the conterminous United States with a discussion on the significance of isostatic residual anomalies: Journal of Geophysical Research, v. 91, p. 8348–8372.
Snyder, D.B., Roberts, C.W., Saltus, R.W., and Sikora, R.F., 1981, Magnetic tape containing the principal facts of about 64,000 gravity stations in the state of California: [Available from National Technical Information Service, Springfield, VA 22161 as NTIS Report PB82–168–287].
Stewart, J.H., and Carlson, J.E., 1978, Geologic map of Nevada: U.S. Geological Survey, scale 1:500,000.
Stokes, W.F., 1963, Geologic map of northwestern Utah: University of Utah, scale 1:250,000.
Sumner, J.S., 1985, Crustal geology of Arizona as interpreted from magnetic, gravity, and geologic data, in Hinze, W.J., ed., The Utility of Regional Gravity and Magnetic Maps: Tulsa, Okla., Society of Exploration Geophysicists, p. 164–180.
Tucci, P., Schmocker, J.W., and Robbins, S.L., 1982, Borehole-gravity surveys in basin-fill deposits of central and southern Arizona: U.S. Geological Survey Open-File Report 82–473, 23 p.
Webring, M., 1981, MINC; A gridding program based on minimum curvature: U.S. Geological Survey Open-File Report 81–1224, 41 p.
Zbur, R.T., 1963, A geophysical investigation of Indian Wells Valley, California: U.S. Naval Ordnance Test Station Technical Publication 2795, 98 p.

Table 1. *Cenozoic density-depth functions*

Depth range (km)	Sedimentary density contrast (g/cm^3)	Volcanic density contrast (g/cm^3)
0–0.2	-0.65	-0.45
0.2–0.6	-0.55	-0.40
0.6–1.2	-0.35	-0.35
>1.2	-0.25	-0.25

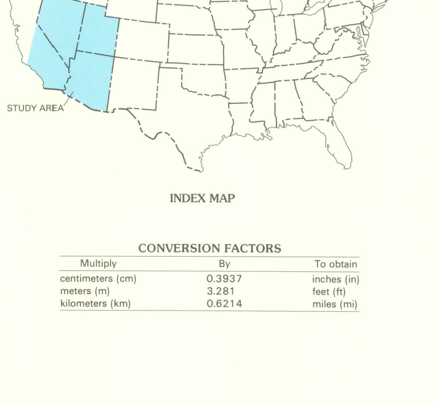

INDEX MAP

CONVERSION FACTORS

Multiply	By	To obtain
centimeters (cm)	0.3937	inches (in)
meters (m)	3.281	feet (ft)
kilometers (km)	0.6214	miles (mi)

GRAVITY AND BASIN-DEPTH MAPS OF THE BASIN AND RANGE PROVINCE, WESTERN UNITED STATES

By
R.W. Saltus and R.C. Jachens

1995

Any use of trade names in this publication is for descriptive purposes only and does not imply endorsement by the U.S. Geological Survey

For sale by U.S. Geological Survey Information Services
Box 25286, Federal Center, Denver, CO 80225